Mathematical modelling of the process of making fireproof protective coverings by two-phase jets*

H. Milosevic, D. Petkovic, N. Kontrec
Faculty of Science and Mathematics University of Pristina, Kosovska Miitrovica, Serbia
e-mail: mhrane@gmail.com, dojcin.petkovic@gmail.com,
natasa_radenkovic@yahoo.com

The mathematical modelling of the process of making fireproof protective coatings reduces to the consideration of a problem of the interaction of a two-phase turbulent jet with a plane wall. The second phase represents a fine-fraction mixture of the coke and magnesite particles, and when impinging on the wall they can both stick to it and reflect from it. The reflected particles near the wall interact with the carrier gas and with the impinging particles thus forming a narrow layer of particles with the increased particles concentration, which is usually called as a screening layer. The computation of such a flow in a jet was performed within the framework of a continual model. For the description of gas flow the averaged Navier — Stokes equation system and $k - \varepsilon$ model of turbulence have been used.

Keywords: numerical modelling, two-phase flows, fireproof protective coatings, combustion of coal particles, steel-melting converters.

Introduction

Two-phase jets are used for making a protective additional coating on the refractory walls of different industrial devices (called as the process of guniting). The guniting of the walls of steel-melting converters is used in Russia [1]. It allows to increase the number of melting's in several times without the replacement of converter's base fire-proof walling and this method give a large commercial profit.

A problem of numerical modelling of this process within the framework of technological scheme with coaxial jets is considered. This technological scheme of the jet guniting is shown in Fig. 1.

Two-phase mixture of burning (coke) and non-burning (magnesite) particles and nitrogen (carrier gas) is fed into the central jet and the peripheral (annular) jet of the oxygen is used for combustion of the coke. The heat releasing from the burning of coke particles results in the increasing of the magnesite particles temperature.

Solid particles have sufficiently small dimensions (of the order 80–100 μm), and when impinging on the wall they can both stick to it and reflect from it. The reflected particles near the wall interact with the carrier gas and with the impinging particles thus forming a narrow layer of particles with the increased particles concentration, which is usually called as a screening layer.

*The work was supported by the Serbian Ministry of Education and Science (project III44006&TP35030).

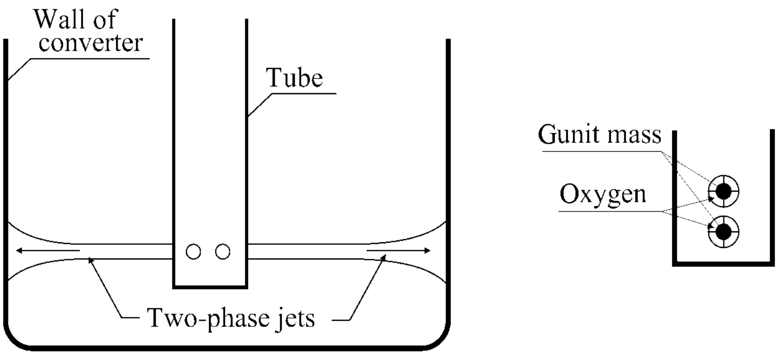

Fig. 1. Technological scheme of the jet guniting

Mathematical model

The sketch computational region of flow is shown in Fig. 2. The peripheral oxygen jet is a high-speed jet, and the central two-phase jet. The jet outflowing from this device has a sufficiently large extension (100–200 calibres), therefore the overall flow region was subdivided into three regions: flow region was subdivided into three regions: the non-isobaric flow region in and near the nozzle device (I), the region of isobaric jet (II), and the region of the interaction of the jet with the converter wall (III), the computation of the flow in which was carried out sequentially. Here the values of flow parameters obtained at the right boundary of each region were the initial data for the computation in the next region.

The simulation of the turbulent two-phase flow was performed within the framework of "$k - \varepsilon$" model taking into account the influence of turbulent pulsations on the motion of particles. The averaged Navier — Stokes model was used for description of motion of carrier gas.

In addition, the following simplifying assumptions were used:

— the flow is stationary and axisymmetric;

— the carrying medium consists of the oxidizer (O_2), reaction products (CO_2) and the inert gas (N_2). The gaseous phase density is determined as $\rho = \rho_1 + \rho_2 + \rho_3$ (here and in what follows the indices of the flow parameters will be denoted by figures from 1 to 5 for O_2,

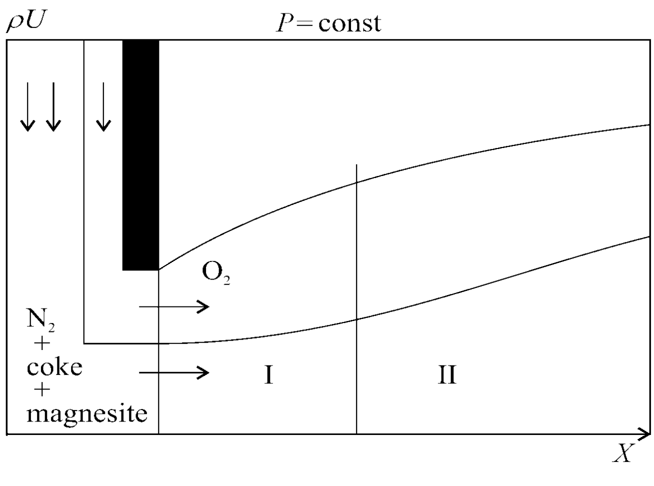

Fig. 2. Diagram of computational region

CO_2, N_2, coke particles and magnesite particles, respectively; the parameters without the indices will refer to the gaseous phase on the whole). The ambient space is filled by a hot air;

— the second phase consists of spherical particles of two kinds — the combustible particles (coke) and non-combustible particles (magnesite). The dimensions of magnesite particles are constant, those of coke are variable at the expense of coke combustion. The reaction between the coke particles and oxygen is one-stage and is described by equation $C + O_2 = CO_2$;

— the reaction takes place only on the surface of a coke particle, and the heat produced thereby is expended for the heating of the particle itself, and then this heat is transferred to the carrying gas and through the gas to the magnesite particles in the result of an interphase heat exchange. The temperature throughout the volume of any particle is the same; in the process of combustion the particle preserves its spherical shape.

The system of equations governing the two-phase stationary flow has the following form (into regions I and II).

$$\frac{\partial}{\partial x_k} y\rho U_k = yJ, \tag{1}$$

$$\frac{\partial}{\partial x_k} y\rho U_i U_k + \frac{\partial}{\partial x_k} yP = \frac{\partial}{\partial x_k} y\left[\mu\tau_{ik} - \rho < u_i^{'} u_k^{'} >\right] + y\left(F_i - JU_{4i}\right), \tag{2}$$

$$\frac{\partial}{\partial x_k} y\rho H U_k = U_k \frac{\partial}{\partial x_k} yP + \frac{\partial}{\partial x_k} y\left[\lambda\frac{\partial T}{\partial x_k} - \rho < h^{'} u_k^{'} > + \left(\mu\tau_{ik} - \rho < u_i^{'} u_k^{'} >\right)\frac{\partial U_i}{\partial x_k}\right] +$$

$$+ y\sum_{m=4}^{5} \rho_m \left\{C_{\alpha m}\left(T_m - T\right) + \left(U_{m1}F_1 + U_{m2}F_2\right)\right\}, \tag{3}$$

$$\frac{\partial}{\partial x_k} y\rho_m U_k = \frac{\partial}{\partial x_k} y\left[\left(\rho D_m + \frac{\mu_T}{Sct}\right)\frac{\partial \rho_m}{\partial x_k}\right] + yJ_m, \quad m = 1, 2, \tag{4}$$

$$\frac{\partial}{\partial x_k} y\rho U_k k = \frac{\partial}{\partial x_k} y\left[\left(\mu + \frac{\mu_T}{\sigma_k}\right)\frac{\partial k}{\partial x_k}\right] - y\left[\rho < u_i^{'} u_k^{'} > \frac{\partial U_i}{\partial x_k} - \rho(\varepsilon + \varepsilon_s)\right], \tag{5}$$

$$\frac{\partial}{\partial x_k} y\rho U_k \varepsilon = \frac{\partial}{\partial x_k} y\left[\left(\mu + \frac{\mu_T}{\sigma_\varepsilon}\right)\frac{\partial \varepsilon}{\partial x_k}\right] - y\left[C_{\varepsilon 1}\frac{\varepsilon}{k}\rho < u_i^{'} u_k^{'} > \frac{\partial U_i}{\partial x_k} - C_{\varepsilon 2}\rho\frac{\varepsilon^2}{k} - C_{\varepsilon 3}\rho\varepsilon_s\right], \tag{6}$$

$$P = TR_0 \sum_{m=1}^{3} \rho_m / g_m, \tag{7}$$

$$\tau_{ik} = \left(\frac{\partial U_i}{\partial x_k} + \frac{\partial U_k}{\partial x_i} - \frac{2}{3}\frac{\partial U_l}{\partial x_l}\delta_i k\right), \quad \rho < u_i^{'} u_k^{'} >= \frac{2}{3}\rho k\delta_{ik} - \mu_T\tau_{ik},$$

$$\mu_T = C_\mu \rho k^2/\varepsilon, \quad \rho < h' u_k' >= -\frac{\mu_T}{\mathrm{Pr}_T}\frac{\partial H}{\partial x_k},$$

$$\frac{\partial}{\partial x_k} y\left(\rho_m U_{mk} + < \rho_m^{'} u_m^{'} >\right) = J_m, \quad m = 3, 4, \tag{8}$$

$$\frac{\partial}{\partial x_k} y\left(n_4 U_{4k} + < \rho_4^{'} u_4^{'} > / \rho_4\right) = 0, \tag{9}$$

$$\frac{\partial}{\partial x_k} y\left[\rho_m U_{mi} U_{mk} + U_{mi} < \rho_m^{'} u_{mi}^{'} > - \rho_m < \rho_{mi}^{'} u_{mk}^{'} >\right] = y\rho_m C_{Rm}(U_i - U_{mi}), \tag{10}$$

$$\frac{\partial}{\partial x_k} y \left[\rho_m U_{mi} H_m + H_m < \rho_m^{'} u_m^{'} > - \rho_m < h_m^{'} u_{mk}^{'} > \right] = y \left[\rho_m C_{\alpha m} (T - T_m) + J_m Q \right], \quad (11)$$

$$J = J_2 - J_1, \quad J_4 = -J, \quad J_5 = 0,$$

where repeated indices imply summation, τ_{ik} is the tensor of viscous stresses, $\rho < \rho_i^{'} u_k^{'} >$ is the tensor of Reynolds stresses, ρ is the calculated density, $\overrightarrow{U}$ is the velocity vector, h is the specific enthalpy, T is the temperature, μ is the dynamic viscosity, μ_T is the turbulent dynamic viscosity, C_R is the coefficient of the aerodynamic drag of a particle, C_α is the coefficient of the heat transfer from the particle to the gas, Pr_T is the turbulent Prandtl number, k is the kinetic energy of turbulence, ε is the rate of its dissipation, J_1, J_2 are the mass rate of expending O_2 and forming CO_2, g_m are the molecular weights of the components, Q is the heat of the coke combustion, n is calculated number of particles per the unit volume. The correlations of the pulsation parameters of particles are determined in terms of the averaged parameters of the carrying gas. The expressions form them, as well as the expressions for C_R, C_α and for the terms ε_s, taking into account the additional dissipation k on particles with regard for their combustion are taken from [2, 3] and are not presented here because of their bulky form. The change of the coke particles radius r_k was determined by the computed values ρ_4 and n_4 with the aid of the formula $r_4 = 3\rho_4/(4\pi\rho c n_4)$, where ρ_c is the true coke density. For the description of a complex process of the coke combustion the expression for its mass rate J_4 was used from [4], which works sufficiently well in the domains of both kinetic and diffusive regimes of combustion.

As the boundary conditions in the inlet section of the nozzle device, for the gas we have specified the values of the mass flux (ρu), the enthalpy and the direction of the velocity vector. For the particles we have specified here the values of all the parameters under the assumption on the absence of their lag in velocity and temperature. On the device wall the sticking conditions were specified for the gas, and the slip conditions were specified for the particles. The conditions typical for the ambient space were specified in the upper boundary and the nonreflecting condition was specified in the outlet boundary.

In the region (I) the system (1)–(11) was replaced by a no stationary system and was solved by the pseudo-unsteady method with the aid of Patankar's method SIMPLE [5], and for the solution of the equations for particles motion the implicit A-stable second-order scheme was used [6]. In the region (I) in the nozzle device the well-known method of near-wall functions was used to determine the values of k and ε near the walls [7].

In the region (II) the pressure was assumed to be constant, and the parabolized system (1)–(11) was considered here, which was solved by a marching method.

Then it was assumed that in the region (III) there are only the magnesite particles and there are not any chemical reactions (in system (1)–(7): $J = J_1 = J_2 = 0$, ρ_1, ρ_2 are constants). The particles reflected from the wall are considered as a new fraction, and they are described by the corresponding equation system. Therefore instead of system (8)–(11) we used following equation system:

$$\frac{\partial}{\partial x_k} y \left(\rho_m U_{mk} + < \rho_m^{'} u_m^{'} > \right) = 0, \quad m = 1, 2, \quad (12)$$

$$\frac{\partial}{\partial x_k} y \left[\rho_m U_{mi} U_{mk} + U_{mi} < \rho_m^{'} u_{mi}^{'} > - \rho_m < \rho_{mi}^{'} u_{mk}^{'} > \right] + G_m \frac{\partial}{\partial x_k} y \rho_i =$$

$$= y \left\{ \rho_m C_{Rm} (U_i - U_{mi}) + \sum_{j=1}^{2} K_{mj} \rho_m \rho_j (U_{ji} - U_{mi}) / (M_j + M_m) \right\}, \quad (13)$$

$$\frac{\partial}{\partial x_k} y \left[\rho_m U_{mi} H_m + H_m < \rho_m^{'} u_m^{'} > - \rho_m < h_m^{'} u_{mk}^{'} > \right] =$$

$$= y \left\{ \rho_m C_{\alpha m}(T - T_m) + \sum_{j=1}^{2} K_{mj} \rho_m \rho_j \Phi_{mj}) / (M_j + M_m) \right\}, \tag{14}$$

$$\Phi_{mj} = |\vec{U}_m - \vec{U}_j|^2/2, \quad K_{mj} = \pi[r_m + r_j]^2 |\vec{U}_m - \vec{U}_j|,$$

where K_{mj} — the constant of particles coagulation, r_m — radius and mass of particles, G_m — solids stress modulus [8]. The subscript 1 refers to the parameters of incident particles, and the subscript 2 refers to the reflected particles.

The boundary conditions on the wall were specified for the reflected particles as follows. It was assumed that the mass, the tangent component of the velocity vector and the particles temperature do not change in the process of their reflection from a wall, and the value of the normal component of the velocity vector was determined from the relationship $u_2 = -\beta u_1$, where β is the accommodation coefficient, which takes into account the inelasticity of the particles collisions with a wall (we have assumed $\beta = 0.2$ in the computations). The ratio of the number of the reflected particles to the number of the incident particles was assumed to be equal to unity, that is a complete reflection of particles was assumed. This has been made with the purpose of determining the maximal protective properties of the screening layer (no less than 80 % of the incident particles are usually reflected).

Some numerical results

The turbulent two-phase flows were calculated with following values of main parameters. All linear dimensions are referred to the radius of the exit section of the annular nozzle ($r_* = 0.015$ m), the velocities of gas and particles are referred to the critical sound speed in the oxygen ($a_* = 298$ m/s), their temperatures are referred to the stagnation temperature, the densities are referred to the stagnation density ($\rho_0 = 1.28$ kg/m). The diameters of the coke and magnesite particles in the inlet section were assumed to be the same ($d_3 = d_4 = 100$ μm), the relation of the mass flow rate of the second phase to the mass flow rate of the carrier gas $W_s/W_g = 10$ ($W_s = W_1 + W_2$), and the weight fraction of coke $q = W_1/W_2$ was varied. The stagnation temperature T_0 for both gases in the inlet section was equal to 300 K, the air temperature in the ambient space was 1700 K.

The computations have shown that under the same conditions the intensity of the two-phase jet expansion is significantly less than in the case of a monophase jet, which is related to the back influence of particles on the gas flow field. In Fig. 3 the flow parameters distributions along the jet axis are shown (the curves *1* correspond to the parameters of the pure gas, and the curves *2* correspond to the two-phase flow, the dashed lines refer to the magnesite particles velocity).

It may be seen that the central jet is accelerated by the viscous interaction with the high speed peripheral jet, and the presence of the second phase reduces the intensity of acceleration. However, in the main region of the jet flow the particles velocity exceeds the gas velocity, and the particles begin to carry the gas along, thus increasing the "range" of the two-phase jet. The increasing of the gas temperature due to the particles combustion occurs at a sufficiently large distance from the mouthpiece. This indicates to a considerable lag of the coke particles ignition process. Filming of the industrial guniting process confirms the obtained results.

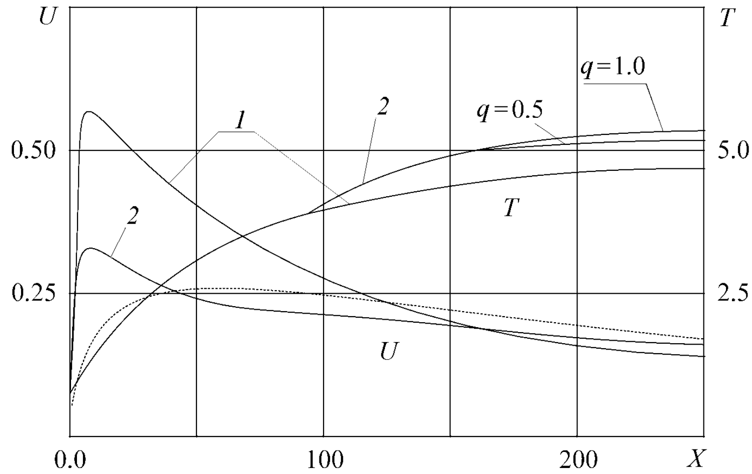

Fig. 3. Flow parameters along the jet axis

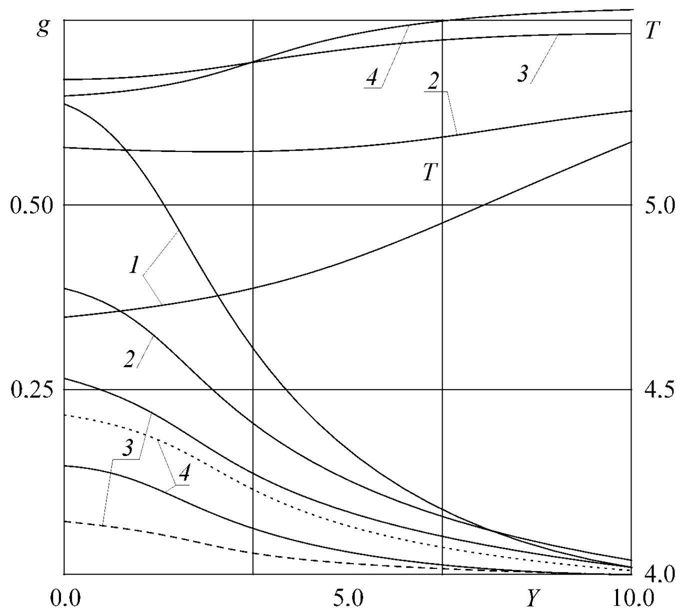

Fig. 4. Flow parameters at $x = 250$. 1 — $q = 0$; 2 — $q = 0.5$; 3 — $q = 1.0$; 4 — $q = 1.5$

In Fig. 4 we show in section $x = 250$ at different values of the parameter q the distributions of the density of magnesite particles (solid lines) and of coke particles (dashed lines), and the gas temperature in the cross section of the jet. With the parameter q increasing, the fraction of non-burnt coke particles also increases, which makes worse the quality of the coating produced by guniting.

In Fig. 5 we depict the distribution of the magnesite particles density along the jet axis for the different regimes of flow (solid lines and dashed lines) and q.

The solid lines and dashed lines denote high-speed and low-speed jet of oxygen, respectively. A sharp increase of the particles density at the initial part of the high-speed jet is related to the effect of the "lacing" of the particles jet, which is expressed by the reduction of the cross dimension of their jet. This effect is conditioned by the influence of turbulent pulsations of the carrier gas on the particles motion.

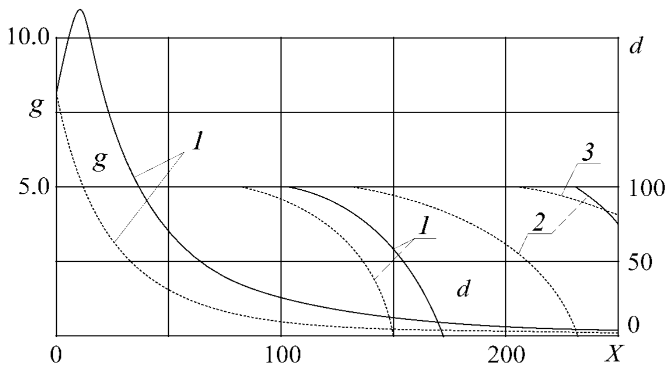

Fig. 5. Density of magnesite particles and the coke particles diameters along the jet. *1* — $q = 0.5$; *2* — $q = 1.0$; *3* — $q = 1.5$

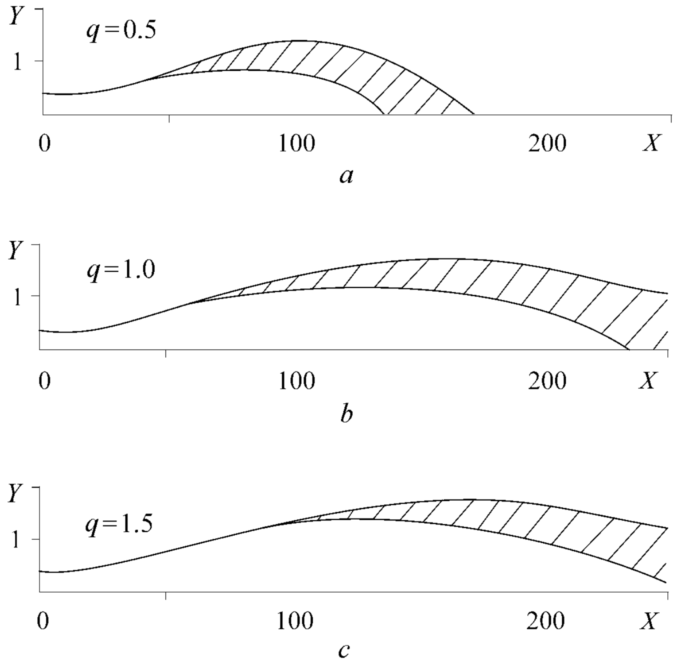

Fig. 6. Zones of the beginning and end of the coke combustion

In the case of low-speed jet the mixing of the jets occurs considerably faster with less intensive generation of k. The consequence of this is the absence of the “lacing” effect. We show in the same Figure the change of the coke particles diameter along the jet axis for three values of the coefficient q, from which it follows that the “lacing” effect reduces the intensity of the coke combustion process.

The dispositions of the zones of the beginning and ending of the coke combustion in the jets are presented in Fig. 6. It may be seen that the increase of the relative fraction of coke in the gunit mass leads to a substantial lag of the combustion process, the intensity of which is limited by a turbulent diffusion of oxygen from the peripheral jet.

In Fig. 7 we show a qualitative picture of the distribution of particles density near the wall surface in the incident jet for the particles with the diameter $d_p = 100$ μm without regard (Fig. 7, *a*) and with regard (Fig. 7, *b*) of the force interaction between the incident and reflected particles. It may be seen that the consideration of such an interaction alters

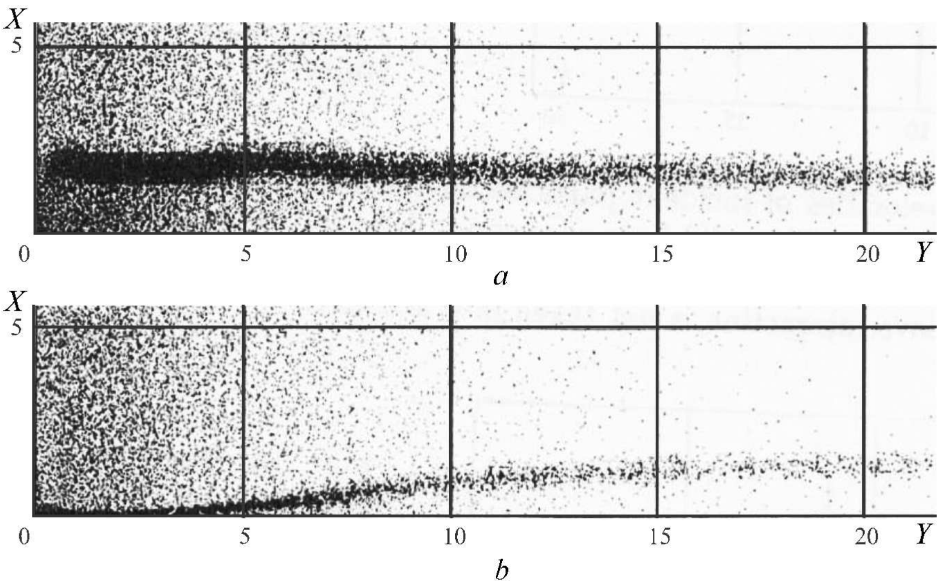

Fig. 7. Distribution of particles density near the wall surface

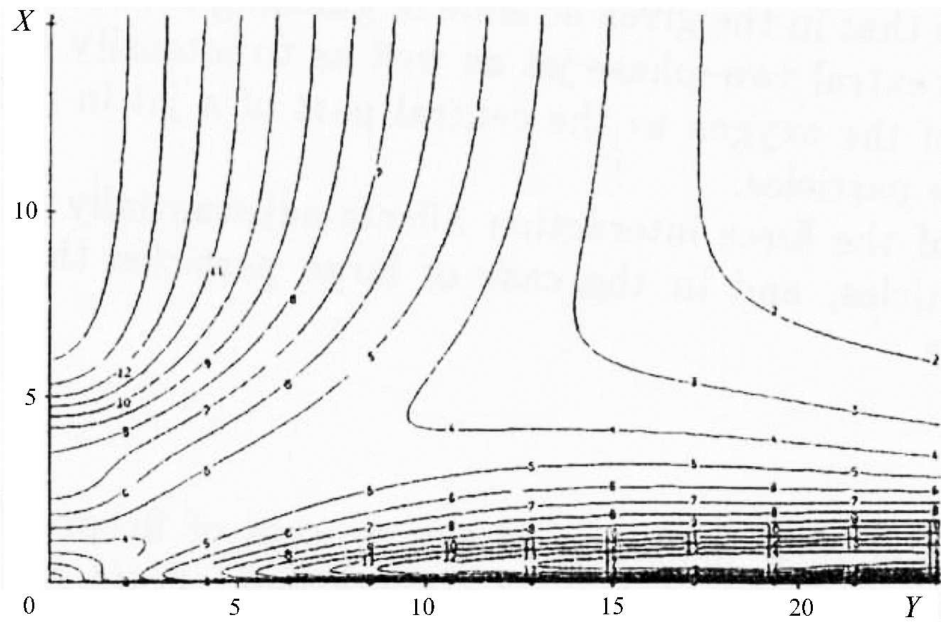

Fig. 8. Isolines of the Mach number

significantly the structure of the screening layer, which now “presses itself” to the wall on the jet axis, where the impinging particles have the largest energy. The isolines of the Mach numbers of the carrying gas are presented in Fig. 8.

One may well see a region of the formation of the boundary layer along the wall. The effect of the particles with $d_p = 100$ μm on the flow structure of the carrying gas is insignificant, and it becomes appreciable in the case of particles of small sizes $d_p \leq 100$ μm.

We show in Fig. 9 the pressure distributions along the wall for the particles with $d_p = 100$ μm and $d_p = 10$ μm. It may be seen that the pressure at the spreading point in the case of $d_p = 10$ μm is higher. That is related with more intensive interaction between carrier gas and particles of the small diameters.

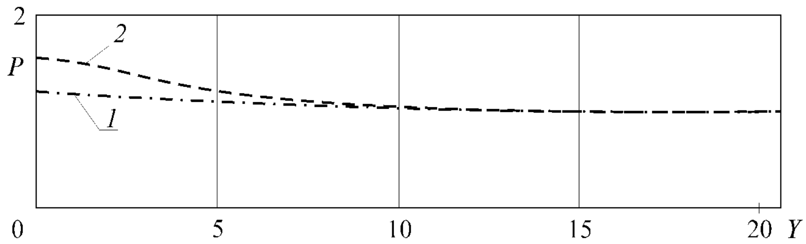

Fig. 9. Presse distribution along the wall. *1* — $d_p = 100$ μm, *2* — $d_p = 10$ μm

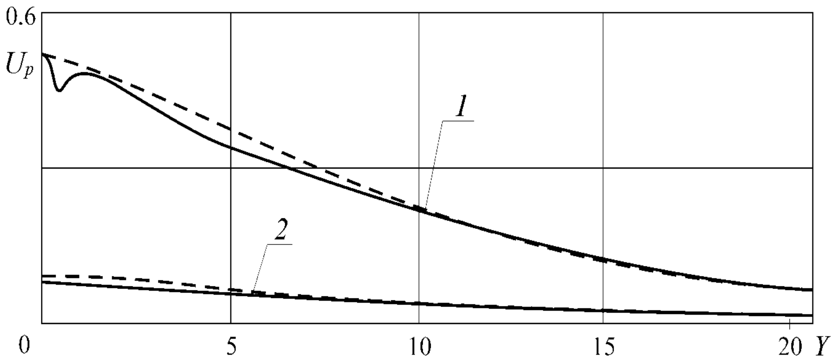

Fig. 10. Distribution of the velocities of incident particles on the wall. *1* — $d_p = 100$ μm, *2* — $d_p = 10$ μm

The distributions of the velocities of incident particles on the wall are depicted in Fig. 10 for $d_p = 100$ μm and for $d_p = 10$ μm. The solid lines correspond here to the computations taking into account the force interaction between the incident and reflected particles. The dashed lines refer to the case when the above interaction is not taken into account.

Conclusion

The analysis of computational results shows that in the given scheme of guniting it is reasonable to provide sufficiently high velocity of the central two-phase jet as well as to intensify in some way the process of the turbulent transfer of the oxygen to the central part of a jet in order to ensure a more complete combustion of coke particles.

It was showed that the consideration of the force interaction affects substantially the distribution of the velocities of incident particles, and in the case of large particles this effect ($d_p = 100$ μm) proves to be even qualitative.

References

[1] Rychkov A.D., Miloshevich H. Numerical modeling of the process of fireproof coating formation by jet coating // Proc. of the First Asian Computational Fluid Dynamics Conference. Hong-Kong, 1995. Vol. 3. P. 1041–1047.

[2] Schreiber A.A., Gavin L.B., Naumov V.A., Yatsenko V.P. Turbulent flows of gas-particles mixtures (in Russian). Kiev: Naukova Dumka, 1987.

[3] Mostafa A.A., Mongia H.C., WcDonell V.G., Samuelsen G.S. Evolution of particle-laden jet flows: a theoretical and experimental study // AIAA J. 1989. Vol. 27. P. 167–183.

[4] Khitrin L.N. Physics of combustion and explosion (in Russian). M.: Publ. by Moscow State Univ. 1957.

[5] Patankar S. Numerical heat transfer and fluid flow. N.Y.: Hemisphere Publ. Corporation, 1980.

[6] Rychkov A.D. Mathematical modeling of gasdynamical processes in channels and nozzles (in Russian). Novosibirsk: Nauka, 1980.

[7] Rodi W. Exam pels of turbulence models for incompressible flows // AIAA J. 1982. Vol. 20. P. 872–879.

[8] Tsuo Y.P., Gidaspov D. Computation of flow patterns in circulating fluidized beds // AIChE J. 1990. Vol. 36, No. 6. P. 885–896.

Received for publication 8 November 2011

ЖВТ. 2012. Т. 17, № 2. С. 3–12.

Математическое моделирование процесса создания противопожарного защитного покрытия с помощью двухфазных струй

Х. Милошевич, Д. Петкович, Т. Контреч

Математическое моделирование процесса создания противопожарного защитного покрытия сводится к рассмотрению проблем взаимодействия двухфазной турбулентной струи с плоской стеной. Вторая фаза представляет мелкодисперсную смесь кокса и магнезитовых частиц, и во время попадания на стену они могут как прилипать к ней, так и отражаться от нее. Отраженные частицы около стены взаимодействуют с несущим газом и набегающими частицами, таким образом, создавая тонкий слой с повышенной концентрацией частиц, который обычно называется экранирующим слоем. Вычисление такого течения в струе было произведено рамках континуальной модели. Для описания течения газа были использованы осредненные уравнения Навье — Стокса вместе с $k-\varepsilon$ моделью турбулентности.

Ключевые слова: численное моделирование, двухфазные потоки, противопожарное защитное покрытие, горение угольных частиц, сталеплавильные конверторы.